

Supporting Information

Potential therapeutic and diagnostic applications of one-step in situ biosynthesized gold nanoconjugates (2-in-1 system) in cancer treatment

Sudip Mukherjee^a, Vinothkumar B^a, Suthari Prashanthi^b, Prakriti Ranjan Bangal^b, Bojja Sreedhar^b, Chitta Ranjan Patra^{*a}

^aCentre for Chemical Biology, ^bInorganic and Physical Chemistry Division, Indian Institute of Chemical Technology, Uppal Road, Tarnaka, Hyderabad - 500607, AP, India

***To whom correspondence should be addressed**

Chitta Ranjan Patra, Ph.D

^aCentre for Chemical Biology

Indian Institute of Chemical Technology,

Uppal Road, Tarnaka, Hyderabad - 500607, AP, India

Tel: +91-9666204040 (Mobile), +91-40-27191809 (O)

Fax: +91-40-27160387

E-mail: crpatra@iict.res.in; patra.chitta@gmail.com

Running title: Formation of AuNPs by *Olax Scandens* leaf

Key words: Colloidal gold nanoparticles, *Olax Scandens*, Green chemistry,

Fluorescence, Cancer, Diagnostics, Therapeutics

1. EXPERIMENTAL PROCEDURES

1.1. Cell viability test using MTT reagent

The MTT assay (3-(4, 5-dimethylthiazol- 2-yl)-2, 5-diphenyl tetrazolium bromide), a colorimetric assay has been used for measuring the activity of enzymes that reduce MTT to formazan dyes, giving a purple color. This assay has been used to determine the cell viability in presence of any cytotoxic potential medicinal agents/nanomaterials. Briefly, we have plated 10,000 cells (counted by haemocytometer) of different cancer cells (A549, MCF-7 and COLO-205) in a 96 well plate for 24 h and then the cells were incubated with *olax* extract, and as-synthesized AuNPs especially AuNP-OX-500 (Experiment number #4 from Table -1) and Au-MUA (chemically synthesized) in dose dependent condition for another 48 h. We have checked the anticancer property of our as prepared DDS in A549, MCF-7 and COLO-205 cell lines. 1 mL of MTT stock solution (concentration 5 mg/mL) was diluted to 10 mL solution using DMEM media and 100 μ L of this MTT solution was added to each well by replacing the media and allowed to incubate for 4 h. After 4 h, the media in each well was replaced by 100 μ L of DMSO-Methanol mixture (1:1 volume ratio) for solubilizing the violet crystal and kept the mixture on the shaker for homogeneous mixture. Finally, the absorbance of the mixture was measured at 570 nm using a microplate reader (Varioskan Flash). All the experiments were carried out in triplicate and the results are expressed as normalized viability = $\{1/\text{Abs}_{\lambda=570}(\text{untreated cells-blank})\} \times \{\text{Abs}_{\lambda=570}(\text{treated cells-blank})\}$.

2. CHARACTERIZATION TECHNIQUES

The as-synthesized AuNPs were thoroughly characterized by several physico-chemical techniques that are described below:

2.1. *UV-VIS spectroscopy*

The absorption of all as-synthesized AuNPs was measured by UV-vis spectroscopy (JASCO dual-beam spectrophotometer (*Model V-570*)) in a quartz cuvette from 800 to 200 nm with a resolution of 1 nm.

2.2. *X-ray diffraction (XRD)*

The structure and phase purity of the as-synthesized AuNPs samples were determined by X-ray diffraction (XRD) analysis using a Bruker AXS D8 Advance Powder X-ray diffractometer (using $\text{CuK}\alpha\lambda=1.5406 \text{ \AA}$ radiation). The red intense loose pellets of as-synthesized AuNPs samples were obtained by centrifugation at a 14,000 rpm at 10^0 C for 1 h in Thermo scientific, Sorvall-WX ultra 100. The glass slide was coated with this loose AuNPs pellet by evaporating the solvent repeatedly and submitted for XRD analysis.

2.3. *Transmission electron microscopy (TEM)*

The morphology and shape of nanoparticles were examined on a FEI Tecnai F12 (Philips Electron Optics, Holland) instrument operated at 100 kV. Selected area electron diffraction (SAED) patterns were also taken using this instrument. Initially, the red intense loose pellet of as-synthesized AuNPs samples were obtained by centrifugation at a 14,000 rpm at 10^0 C for 1 h and diluted with water (1:3 ratio). Samples for TEM

analysis were prepared by placing a drop of this diluted loose pellet solution on carbon-coated copper grid and allowed the grid to evaporate the solvent.

2.4. Inductively coupled plasma optical emission spectrometry (ICP-OES)

An inductively coupled plasma optical emission spectrometer (ICP-OES, IRIS intrepid II XDL, Thermo Jarrel Ash) was used to determine the concentrations of gold ions in the aqueous solutions. Initially, a series of standard HAuCl_4 solution with concentration range of 5-50 ppm was prepared for gold standard curve. Then we have calculated the concentration of gold ion in AuNP-Ox-500 and cAuNP-MUA (chemically synthesized AuNP conjugated with mercapto undecanoic acid: MUA) from ICP-OES analysis using this standard curve.

2.5. Fourier transformed infrared spectroscopy (FTIR)

FTIR measurements were carried out to identify the possible functional groups in biomolecules (from plant extract) responsible for the synthesis of AuNPs. The fourier transformed infrared (FTIR) spectra were recorded using thermo Nicolet Nexus 670 spectrometer in the diffuse reflectance mode at a resolution of 4 cm^{-1} in KBr pellets. The red intense loose pellet of as-synthesized AuNPs samples were obtained by centrifugation at a 14,000 rpm at 10^0 C for 1 h in Thermo scientific, Sorvall-WX ultra 100. The glass slide was coated with this loose AuNPs pellet by evaporating the solvent repeatedly and submitted for FTIR analysis.

2.6. Dynamic light scattering (DLS)

The hydrodynamic radius of as-synthesized nanoparticles was calculated from a Dyana Pro; Nanostar, Wyatt. 100 μL of as-synthesized AuNPs solution was taken in the sample chamber for the measurement of the size. Zeta potential of AuNPs solution was measured

in zeta potential analyzer (HORIBA SZ-100) using quartz cuvette taking 20 μL of AuNPs in 1mL of deionized water.

2.7. Fluorescence Correlation Spectroscopy (FCS)

All FCS experiments were performed in home-built instrument where samples were excited by 532 nm (PHOTOP, GDML-5020F) green laser. The laser beam was focused into the sample through an objective lens (Olympus 60X, NA 1.20, water immersion). The fluorescence from the sample was collected by the same objective lens and refocused to the image plane by an achromatic lens (AC254-150-A1, THORLAB, USA) after separation from excitation laser light using dichroic mirror (XF2016, 560DCLP, Omega Optical Inc, Vermont, USA). The isolated fluorescent signal was collected on confocal point by a multimode fiber (radius 100 μm) and other end of the fiber was fed into the input of an avalanche photodiodes (APD) (SPCM-AQRH-13-FC, Perkin-Elmer Optoelectronic, Canada) which detects the signal. The output signals of APD were processed by autocorrelator (FLEX99OEM-12D, Correlator.com, USA) card and correlated data were collected with home-built routine which runs under Lab VIEW (National Instruments). Correlation curves were fitted with single component autocorrelation function to extract diffusion time.

The hydrodynamic radius of the gold nanoparticles were measured by Fluorescence Correlation Spectroscopy

2.8. Gel electrophoresis (SDS PAGE)

In order to find out the specific *olax* proteins responsible for the formation and stabilization of gold nanoparticles, we have carried out 12% SDS-PAGE (sodium dodecyl sulfate-polyacrylamide gel electrophoresis) where we have loaded the concentrated part

of the supernatant of AuNP-OX-500 after centrifugation at 10⁰ C for 1h at 14 k rpm and the water extract of olax leaves. The concentrated extract and supernatant of AuNP-Ox-500 were mixed with one third of 4x laemmli sample loading buffer (Rainbow) with 2-mercaptoethanol (Sigma) and were heated at 100 °C for 5 mins before loading and 50 µL of this mixture was loaded in 12% SDS-PAGE. A standard protein molecular weight marker (BIORAD) was loaded in separate well. Finally, the gel was stained with silver nitrate according to standard protocol and scanned with an Epson 4990 photo scanner (Gel doc).

2.9. Photoluminescence spectra (PL) for Olax and AuNP-Ox-500 by spectrofluorometer

In order to check the fluorescence property we have performed the fluorescence spectroscopy (Fluorolog-3 spectrofluorometer of Horiba Jobin Yvon) to check the fluorescence of *Olax* and AuNP-OX-500 using the *Olax and as synthesized colloidal AuNP-OX-500*.

2.10. Fluorescence imaging for Olax and AuNP-OX-500 by fluorescence microscopy

A549 and MCF-7 cells were cultured at 2x10⁴ cells/ml/well in a 24-well plate for 24 hours at 37 °C incubator with 5% CO₂ in DMEM media. After 24 hours, the cells were incubated with *Olax* and AuNP-OX-500 for another 48 hours. The cells were extensively washed with DPBS for 6 times to remove the *Olax* and AuNP-OX-500 from the surface of cell membrane. Finally, the fluorescence images of *Olax* and AuNP-OX-500 and cancer cells (A549 & MCF-7) treated with *Olax* and AuNP-OX-500 were monitored by an Olympus Fluorescence Microscope through excitation of 518nm (green) and emission of 605nm (Red).

3. RESULTS AND DISCUSSION

3.1. Fluorescence Correlation Spectroscopy (FCS)

Fluorescence Correlation Spectroscopy (FCS) was also used to correlate the size of nanoconjugates. The hydrodynamic radius of AuNP-OX-500 was measured by one-photon luminescence, which has been used to measure the unconstrained Brownian motion and the size of gold nanoparticles through FCS according to our earlier report.¹ The normalized autocorrelation function $G(\tau)$ of the concentration $C(t)$ of solute fluorescent species in a small open volume of a dilute solution is defined as the time average of the product of fluctuations of the detected fluorescence $[\delta F(t)]$ at time t and fluctuation at delayed times $t+\tau$, normalized by the squared time average of the fluorescence emission $[F(t)]$

$$G(\tau) = \frac{\langle \delta F(t) \delta F(t+\tau) \rangle}{\langle F(t) \rangle^2} \quad (1)$$

$$G(\tau) = \frac{1}{V_{\text{eff}} \langle C \rangle} \left(1 + \frac{\tau}{\tau_D} \right)^{-1} \left(1 + \left(\frac{r_0}{z_z} \right)^2 \frac{\tau}{\tau_D} \right)^{-1/2} \quad (2)$$

Upon manipulation of calibrated values for the radial and axial dimensions, r_0 and z_z of the excitation volume (V_{eff}), a fit of eq (2) to the experimental autocorrelation curve gives the average residence time τ_D as well as local concentration of particles $1/V_{\text{eff}} = G(0)$. The diffusion constant D and hydrodynamic radius R_h are then calculated according to:

$$\tau_D = \frac{r_0^2}{4D}$$

$$D = \frac{kT}{6\pi\eta R_h}$$

Where, η is the solvent viscosity, k the Boltzmann constant, and T the temperature. Since, experimental set up influences the size of confocal volume; we therefore used to perform autocorrelation studies with dilute (nM) aqueous solution rhodamine B before actual measurements to calibrate r_0 and to convert diffusion time to hydrodynamic radius. The diffusion coefficient and hydrodynamic radius of rhodamine B in water are considered to be $4.26 \times 10^{-6} \text{ cm}^2\text{s}^{-1}$ and $0.78 (\pm 0.15) \text{ nm}$ respectively at 25°C for calibration.

$$\tau_{D1} = \frac{r_{01}^2}{4D_1} \quad \& \quad \tau_{D2} = \frac{r_{02}^2}{4D_2}$$

$$\frac{\tau_{D1}}{\tau_{D2}} = \frac{r_{01}^2}{r_{02}^2}$$

$$\frac{70 \times 10^{-6}}{1.29 \times 10^{-3}} = \frac{0.78 \text{ nm}}{r_{02}}$$

$$r_{0(AuOX)} = 14.3 \text{ nm} \pm 2 \text{ nm}$$

SIZE: $\sim 28.6 \text{ nm} \pm 4 \text{ nm}$.

3.2. Dynamic light scattering (DLS) technique

The hydrodynamic radius of AuNPs-OX of all experiments (Expt.# 1 to Expt. #4) have been measured by Dynamic light scattering (DLS) method shows that there are almost no differences in the sizes AuNPs-OX, obtained from different experiments. The average hydrodynamic sizes of AuNPs-OX are in the range of 15-165 nm, higher than that of the diameter obtained from TEM. In order to determine the exact size and shape of AuNPs-Olax, images of gold nanoparticles have been taken by TEM. Because of the presence of some larger nanoparticles, surface coated AuNPs-OX with phytochemicals, proteins, flavonoids, carbohydrates and acids,² the hydrodynamic size of AuNPs-Olax (measured by DLS) is obtained in the range of 15-165, which is not the exactly matching with TEM images (Table-1).

Table-1: Size determination of AuNPs-OX by TEM and size and charge determination by DLS

Sample Name	Size from DLS (diameter in nm)	Size from TEM (nm)	Zeta potential Charge (mV)
Olax-AuNps-150 μ L	15-155	5-50	- 15.5 \pm 4.6
Olax-AuNps-400 μ L	10-155	5-55	- 18.2 \pm 6.3
Olax-AuNps-500 μ L	15-165	5-45	- 18.4 \pm 5.3
Olax-AuNps-750 μ L	25-165	5-50	- 15.0 \pm 5.7

However, TEM is direct proof of exact shape and size of nanoparticles. SI-Fig.6.a-d shows the DLS size distribution of the AuNPs-OX obtained by different volume of Olax leaf extract. Since zeta potential (ξ) is a very important tool to check the long-term stability and tendency of aggregation of the as synthesized AuNPs-OX,³ therefore, zeta

potential (ξ) value of all the four sets of AuNPs-OX have measure and presented in Table-1. The negative ξ values of all AuNPs-OX (e.g. AuNP-OX-500 $\xi = -18.4 \pm 0.3$) indicate strong long-term stability and dispersity of the biosynthesized AuNPs-OX.

3.3 Fourier transformed infrared (FTIR) spectroscopy

Numerous published literature support the role of the possible functional groups of phytochemicals or proteins present in the Olax leaf, which help in the reduction of HAuCl_4 to gold nanoparticles and its stabilization. In order to find out the possible functional groups present in the Olax leaf extract, FTIR spectroscopy has been carried out. SI-Fig.7.a and SI-Fig.7.b indicate the FTIR spectra of Olax leaf extract (OX) and AuNPs-OX-500, respectively. The major stretching frequencies obtained from Olax extract are 3384.31, 2922.86, 2853.11, 1738.01, 1608.72, 1512.18, 1461.37, 1258.79, 1074.66, 1034.62, 823.60 and 645.59 cm^{-1} (curve-a in Fig.4) whereas IR peaks at 3421.01, 2923.46, 2852.98, 1737.14, 1629.09, 1460.00, 1376.61, 1162.16, 1071.30 and 532.55 cm^{-1} of AuNP-OX-500 are shown in curve b of SI-Fig.7

The major IR spectrum mainly at $\nu = 1738.01 \text{ cm}^{-1}$ arises due to the C=O stretching modes of aldehydes or ketones in curve-a which shifts to 1734.14 cm^{-1} in curve-b which may be due to C=O stretching modes of acids³⁰ suggesting the role of some aldehydes or ketones in the reduction of HAuCl_4 for the formation and stabilization of AuNPs. On the other hand, IR spectrum at $\nu = 1512.18 \text{ cm}^{-1}$ and $\nu = 1258.79 \text{ cm}^{-1}$ (curve-a) due to the presence of amide II and amide III in proteins of *Olax Scandens* leaves⁴ is disappeared in curve-b (AuNP-OX-500) may be due to the involvement of those proteins for the reduction of HAuCl_4 during the synthesis of AuNPs. The remaining IR peaks in curve -a and -b remain almost unchanged. The role proteins in the reduction and stabilization are

further confirmed by SDS gel electrophoresis (discussed later). The peak at $\nu = 3384.31 \text{ cm}^{-1}$ in curve-a is due to the O-H stretching modes present in the several polyphenols like otacosanol, B-sitosterol in the Olax leaf extract.⁵ Hence, there is a possibility of proteins, alcohols and aldehydes present in the Olax leaf extract that are responsible for the formation and stabilization of AuNPs.

3.4. Silver nitrate staining:

To further check the role of proteins present in Olax leaf extract for the formation of AuNPs by the reduction of HAuCl₄ solution and the stabilization of AuNPs, SDS-PAGE gel run electrophoresis has been carried out where we have used concentrated Olax leaf extract and concentrated supernatant of AuNP-OX-500 as the two samples. Lane-1 of SI-Fig.8 it protein expression around ~15-17 kDa, which is almost disappeared in lane-2 where we have used the concentrated supernatant of AuNP-OX-500, obtained after centrifugation suggesting the role of some low molecular weight proteins (~15-17 kDa) present in Olax leaf extract responsible for formation and stabilization of AuNPs-OX. Our results support the previously reported literature where many researchers have shown that the phenolic compounds, proteins, sugars and amino acids present as the phytochemicals that play an important role for the formation and stabilization of as synthesized AuNPs.^{3,6-9} Although here the protein expression is not too prominent suggesting the minimum involvement of proteins for the formation and stabilization of AuNPs-OX. However, FTIR results support our hypothesis.

3.5. *In vitro* stability studies of AuNPs-OX-500

Stability of nanoparticles or nanoconjugates is very important step for drug delivery in cancer therapy. Therefore, the *in vitro* stability of AuNP-OX-500 (Expt. No. # 3, in

Table-1) have been performed in different types of biological fluids and buffer solutions including DPBS, 5% -10% NaCl solution, buffer saline with pH = 6, 7 & 8, fetal bovine serum (FBS). Briefly, 200 μL of different buffer solutions or biological fluids have been added to the 800 μL of as synthesized AuNP-OX-500 (obtained after 24 hours incubation) and allowed to incubate the mixture for 24 h to 14 days. The absorbance of the corresponding solution has been measured by UV visible spectroscopy at 24 h and 14 days. A slight variation in absorbance or plasmon wavelength (λ_{max}) and plasmon bandwidth ($\Delta\lambda$) (less than 5 nm) have been observed in the 24 h AuNPs-OX-500 sample with respect to 14 days AuNPs-OX-500 (Fig.3.a). These results suggest the *in vitro* stability of AuNPs-OX-500 towards buffers or biological fluids, also supported by published reports.^{3,10} *In vitro* stability of nanoparticles and nanoconjugates on dilution is a vital point for biomedical applications where we require lower concentrations of nanoparticles/nanoconjugates. In this context, *in vitro* stability test of AuNPs-OX-500 has been carried out where as synthesized AuNPs-OX-500 was diluted by 0.2 mL of Mili-Q water in successive steps. The plasmon wavelength (λ_{max}) and plasmon bandwidth ($\Delta\lambda$) after each addition of water have been monitored. According to Lambert-Beer law the absorption intensity should be linear with the concentrations. Consequently, we have found that at $\lambda_{\text{max}} = 532$ nm, the absorption is showing linear dependence with changing the concentration of AuNPs (SI-Fig.9). Also the λ_{max} and $\Delta\lambda$ did not change significantly on dilution from 10^{-5} M to 10^{-6} M suggesting extra stability of AuNPs-OX-500.^{3,10} The reason for extra stability may be due to the presence of several proteins, flavonoids (phenolic compounds), carbohydrates, acids like oleanolic acid, B-sitosterol, oleanolic acid and the glucosides of B-sitosterol and oleanolic acid etc. present in the

Olax leaf extract that provide extra stability of AuNPs-OX-500 by surface coating and protect from aggregations. Because of long-term stability of green synthesized AuNPs-OX-500, it may be very much useful for drug delivery and other biomedical applications.

3.6. Quantification of Olax in AuNPs-OX-500 by UV Vis Spectroscopy

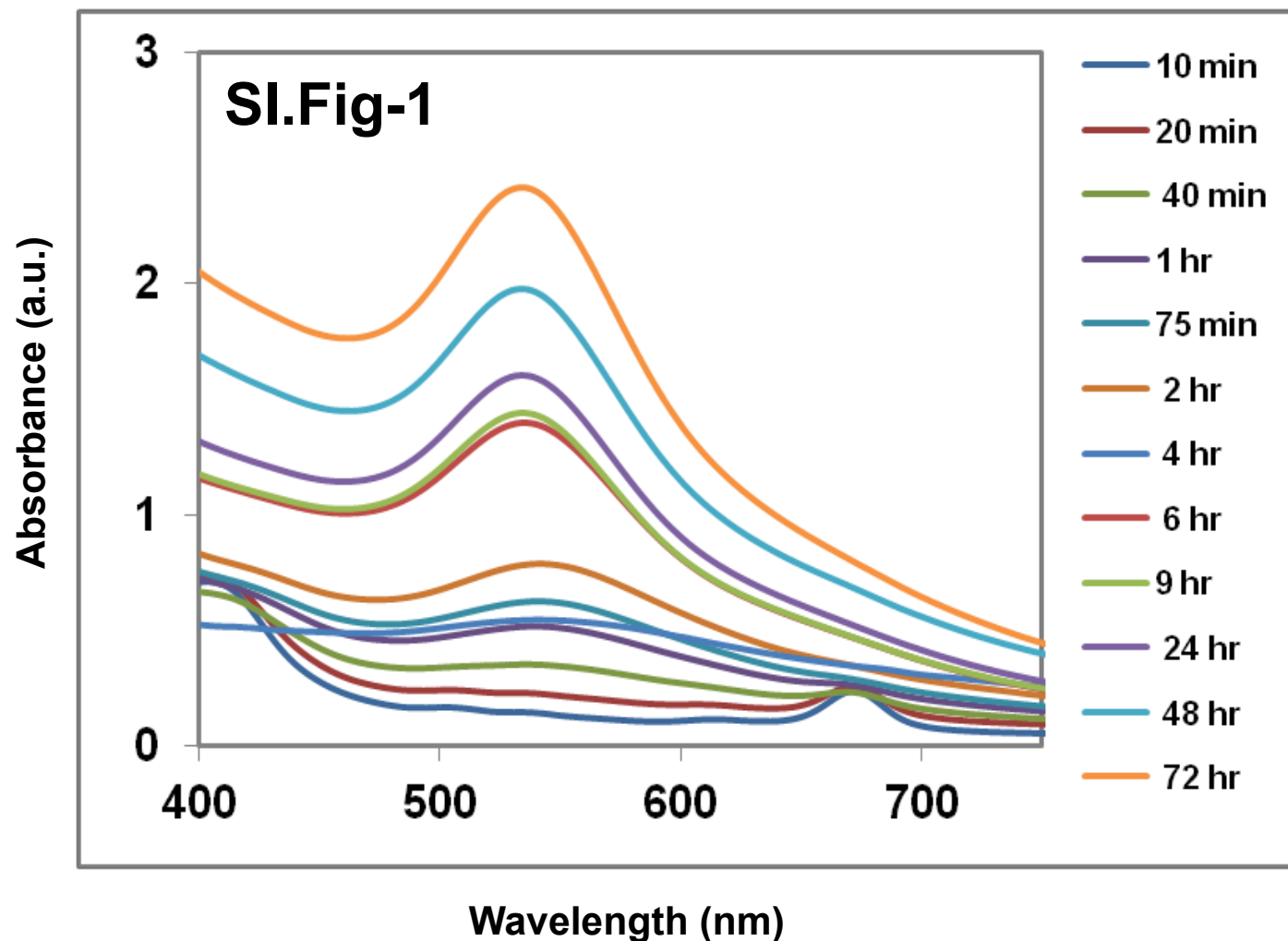
The anti-proliferative effect of Olax leaf extract in cancer cells may be due to the presence of phytochemicals that acts as anti-cancer agent. Therefore, it is necessary to quantify the amount of olax present in the AuNPs-OX-500 after conjugation with AuNPs. Since this Olax leaf extract helps to form and stabilize the AuNPs, therefore we hypothesized that our as synthesized gold nanobioconjugates (AuNPs-OX-500) should contain some phytochemicals that show more anticancer effect in conjugated form. Since the extract shows very interesting absorption properties, therefore the amount of Olax present in AuNPs has been quantitatively estimated by UV vis spectroscopy. Olax leaf extract having two distinct absorption peaks at $\lambda_{\text{max}} = 402.5$ nm and $\lambda_{\text{max}} = 670.0$ nm, therefore we have made a series of solutions with Olax extract in the concentration range of 0.1 mg/mL to 1.5 mg/mL in water and measured the UV-vis spectroscopy (SI-Fig.13). We have plotted two standard curves for Olax by plotting the absorbance vs concentration at $\lambda_{\text{max}} = 402.5$ and 670.0 nm and shown in (Fig.5). From this standard curve, we can measure the concentration of Olax leaf extract from unknown solution.

In order to find out the amount of olax conjugated with AuNPs-OX-500 according to Expt. No. # 3 (Table-1) where we have synthesized 100 ml of AuNP-OX-500 using total amount of 100 mg of Olax. The 100 mL solution was centrifuged at 14,000 r.p.m, 10 °C for 1 h and we have collected 4 mL of loose pellet of AuNP-OX-500 and rest of the solution as colorless supernatant (indicating absence of AuNPs in the supernatant). It is to

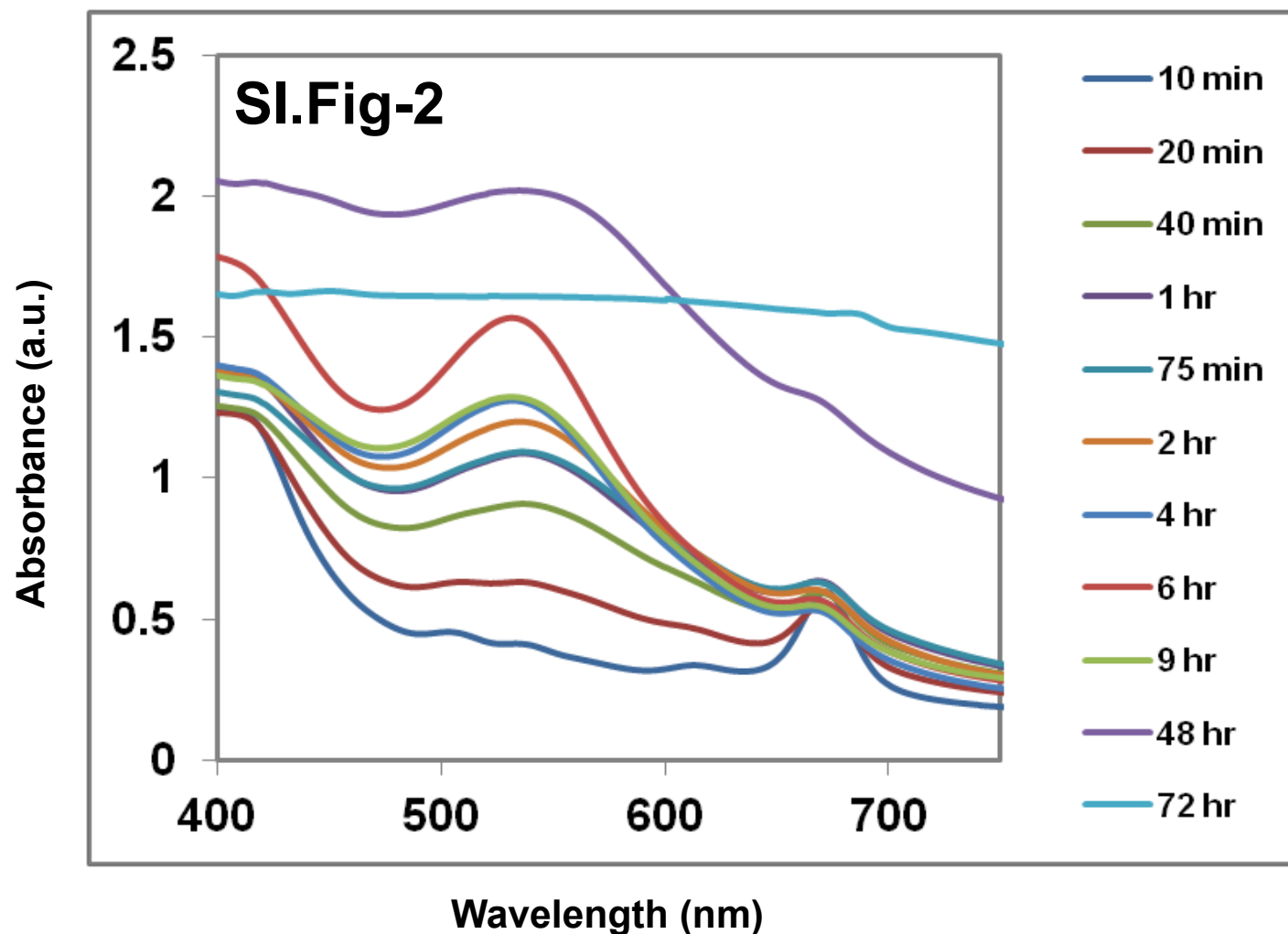
be noted that the loose pellet of AuNPs-OX-500 will be used to check the cell viability in different cancer cells using MTT assay. We have measured the absorbance of the supernatant of AuNP-OX-500 at $\lambda_{\text{max}}=402.5$ and 670.0 nm using UV visible spectroscopy and compare the absorbance values with the standard curve that shows ~ 40% of attachment of Olax in AuNPs-OX-500 (Fig.5 and SI-Fig.14). Hence total 4 mL loose AuNPs-OX-500 pellet (used for cell culture experiments after UV irradiation) contains 40 mg Olax i.e 10 mg/mL.

References:

1. S. Prashanthi, S. R. Lanke, P. H. Kumar, D. Siva and P. R. Bangal, *Appl Spectrosc.*, 2012, **66**, 835-841.
2. A. Balakrishna, N. R. K. and K. K. Purushothaman, *Bmebr*, 1983, **4**, 167-169.
3. R. Shukla, K. S. Nune, N. Chanda, K. Katti, S. Mekapothula, R. R. Kulkarni, V. W. Welshons, R. Kannan and V. K. Katti, *Small*, 2008, **4**, 1425-1436.
4. S. S. Shankar, A. Ahmad, R. Pasricha and M. Sastry, *J. Mater. Chem.*, 2003, **13**, 1822-1826.
5. Z. Krpetic, G. Scari, C. Caneva, G. Speranza and F. Porta, *Langmuir*, 2009, **25**, 7217-7221.
6. J. Xie, Y. J. Lee, I. C. D. Wang and P. Y. Ting, *Small*, 2007, **3**, 672-682.
7. S. K. Bhargava, J. M. Booth, S. Agrawal, C. P. and G. Kar, *Langmuir*, 2005, **21**, 5949-5956.
8. K. A. Wilson, B. R. Rightmire, J. C. Chen and A. I. Tan-wilson, *PlantPhysiol.*, 1986, **82**, 71-76.
9. X. L. Zhu, Q. L. Yang, J. Y. Huang, I. Suzuki and G. X. Li, *Journal of Nanoscience and Nanotechnology*, 2008, **8**, 353.
10. K. S. Nune, N. Chanda, R. Shukla, K. Katti, R. R., R. R. Kulkarni, S. Thilakavathy, S. Mekapothula, R. Kannan and V. K. Katti, *J. Mater. Chem.*, 2009, **19**, 2912-2920.

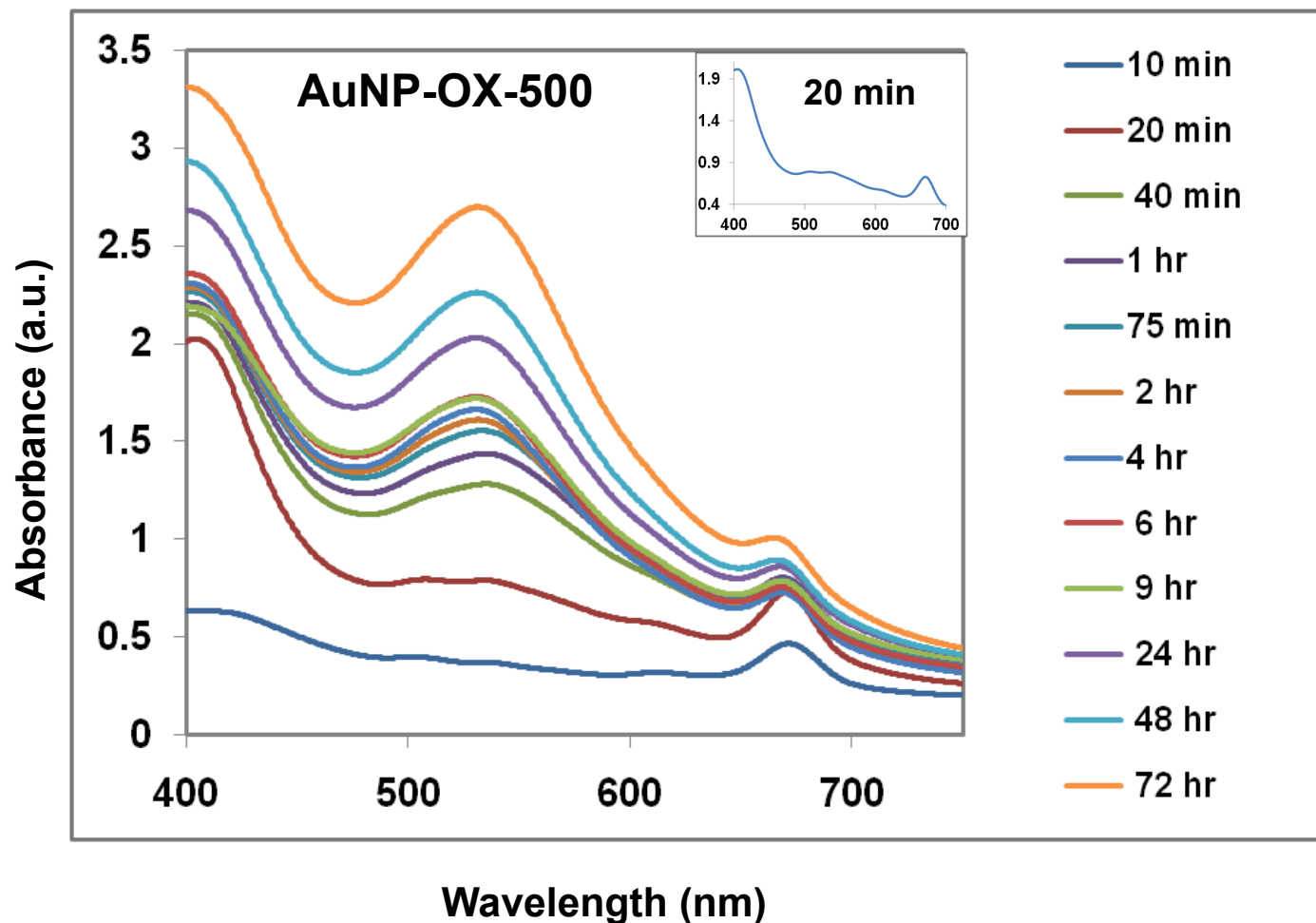


SI.Fig-1: UV visible spectra of gold nanoparticle synthesized by Olax (AuNP-Ox-150) at different time interval. Change of absorbance of as-synthesized AuNP-Ox-150 (Expt. No. #1 in Table-1) with time (1 min to 72 h) indicates that absorption intensity of AuNPs increases with time suggesting the formation of more AuNPs.

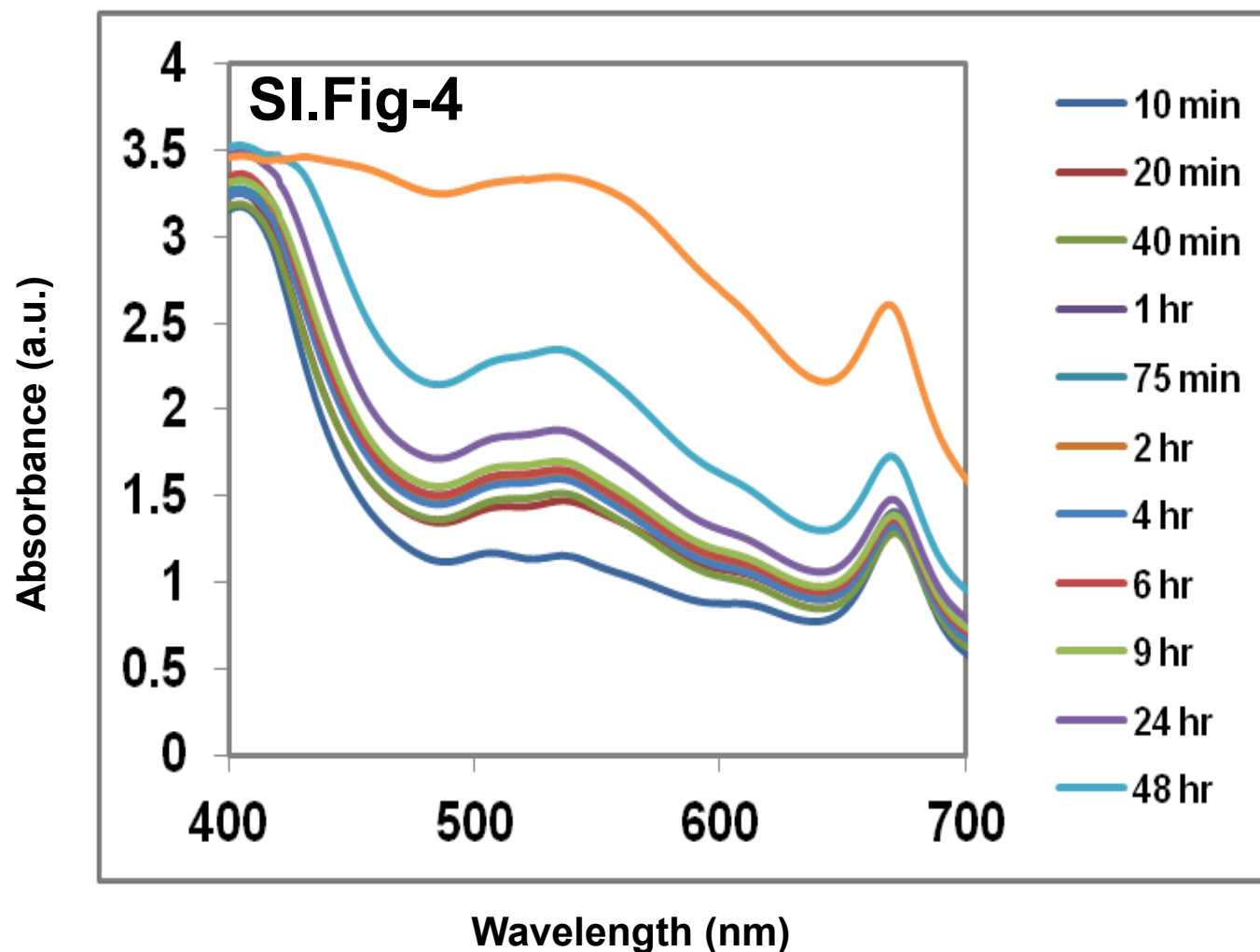


SI.Fig-2: UV visible spectra of gold nanoparticle synthesized by Olax (AuNP-Ox-400) at different time interval. Change of absorbance of as-synthesized AuNP-Ox-400 (Expt. No. #2 in Table-1) with time (1 min to 72 h) indicates that absorption intensity of AuNPs increases with time suggesting the formation of more AuNPs. But at 72 hours the absorbance of AuNP-Ox-400 decreases suggesting the instability.

SI.Fig-3

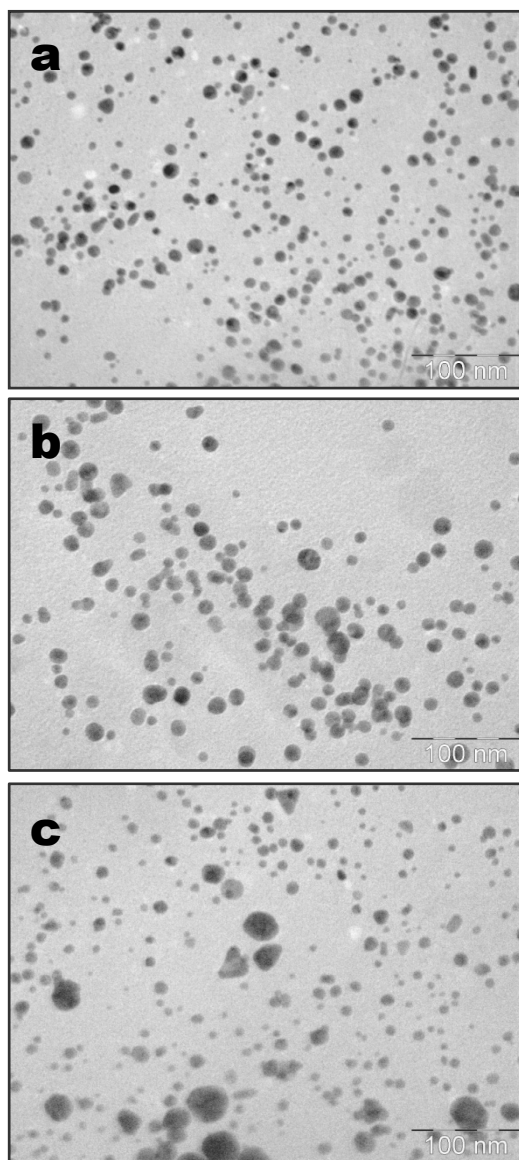


SI.Fig-3: UV visible spectra of green synthesized gold nanoparticles (AuNPs-OX) at different reaction conditions Change of absorbance of as-synthesized AuNP-OX-500 (Expt. No. #3 in Table-1) with time (10 min to 72 h). The pictures show that absorption intensity of AuNPs-OX increases with time suggesting the formation and accumulation of more AuNPs-OX.



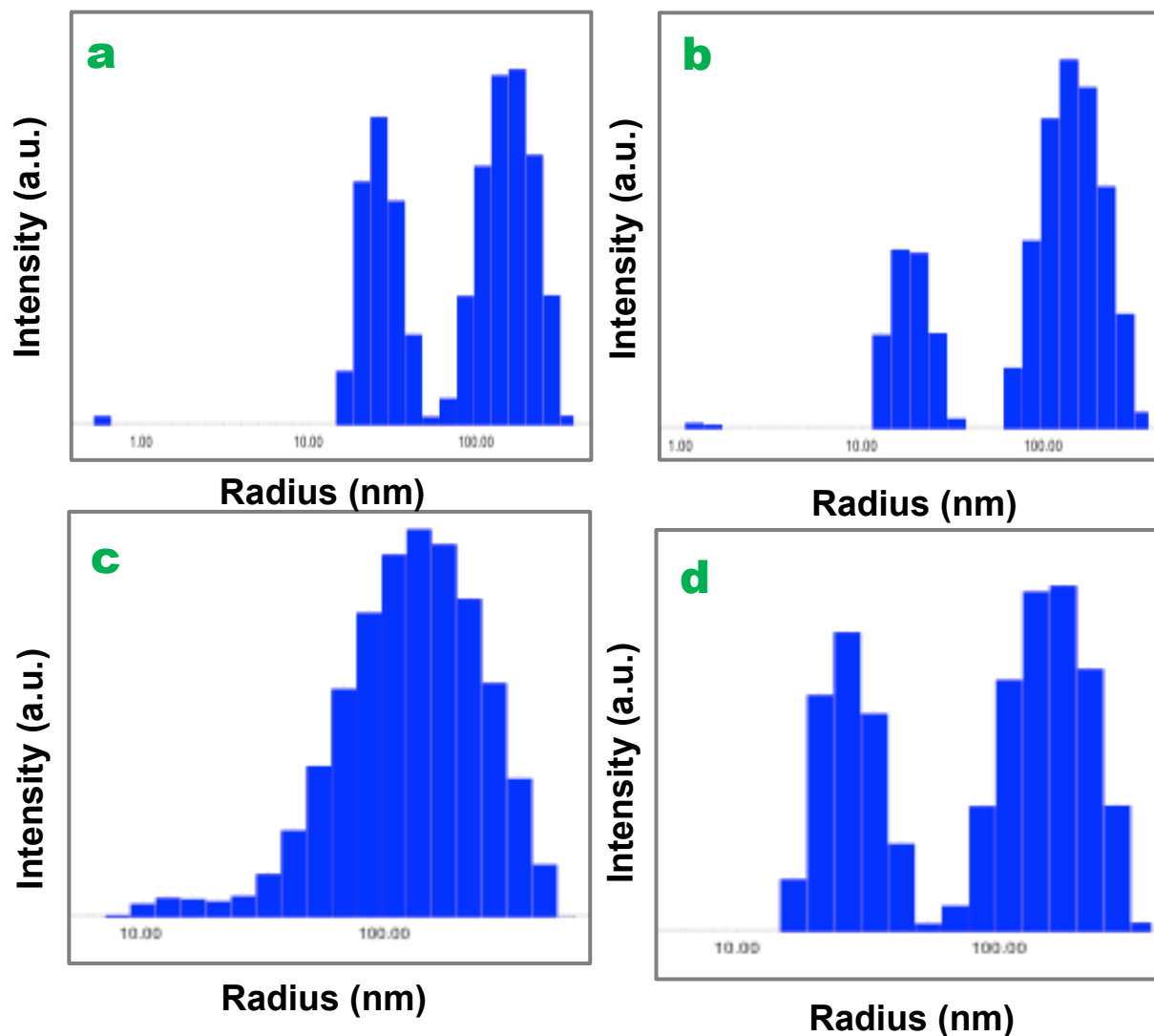
SI.Fig-4: UV visible spectra of gold nanoparticle synthesized by Olax (AuNP-Ox-750) at different time interval. Change of absorbance of as-synthesized AuNP-Ox-750 (Expt. No. #4 in Table-1) with time (1 min to 72 h) indicates that absorption intensity of AuNPs increases with time suggesting the formation of more AuNPs. But the nature of the peaks is not good as other samples.

SI.Fig-5



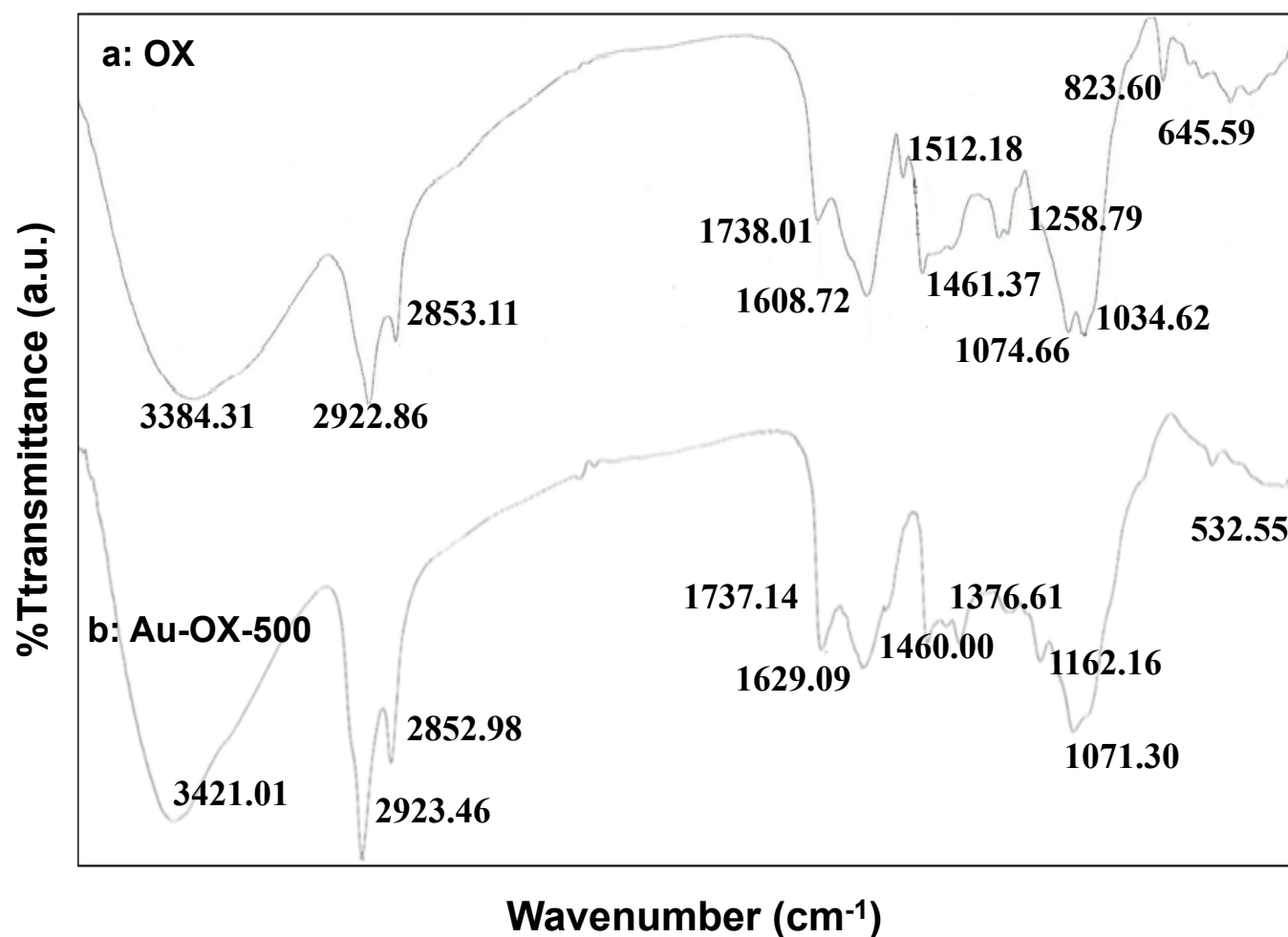
SI.Fig-5: Size and shape of AuNP-Ox-500 in different time interval by TEM. (a) TEM images of AuNP-Ox-500 at 1 day, (b) TEM images of AuNP-Ox-500 at 7 days and (c) TEM images of AuNP-Ox-500 at 14 days suggesting the size of mainly spherical AuNPs slowly increase with time. Also very few triangular AuNPs generate.

SI.Fig-6



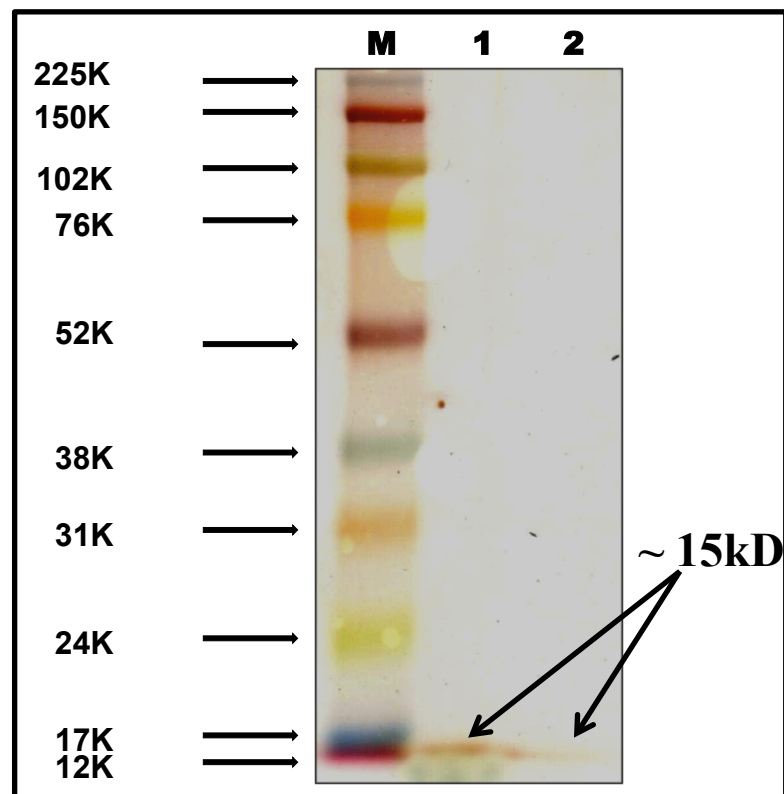
SI.Fig-6: Size distribution pattern of different sets of AuNPs by DLS. (a) DLS size distribution patterns of AuNP-Ox-150, (b) DLS size distribution patterns of AuNP-Ox-400 (c) DLS size distribution patterns of AuNP-Ox-500 and (d) DLS size distribution patterns of AuNP-Ox-750 suggesting the monodispersity of spherical AuNPs for AuNP-Ox-500, but not so much high monodispersity for other sets of as synthesized AuNPs.

SI-Fig.7



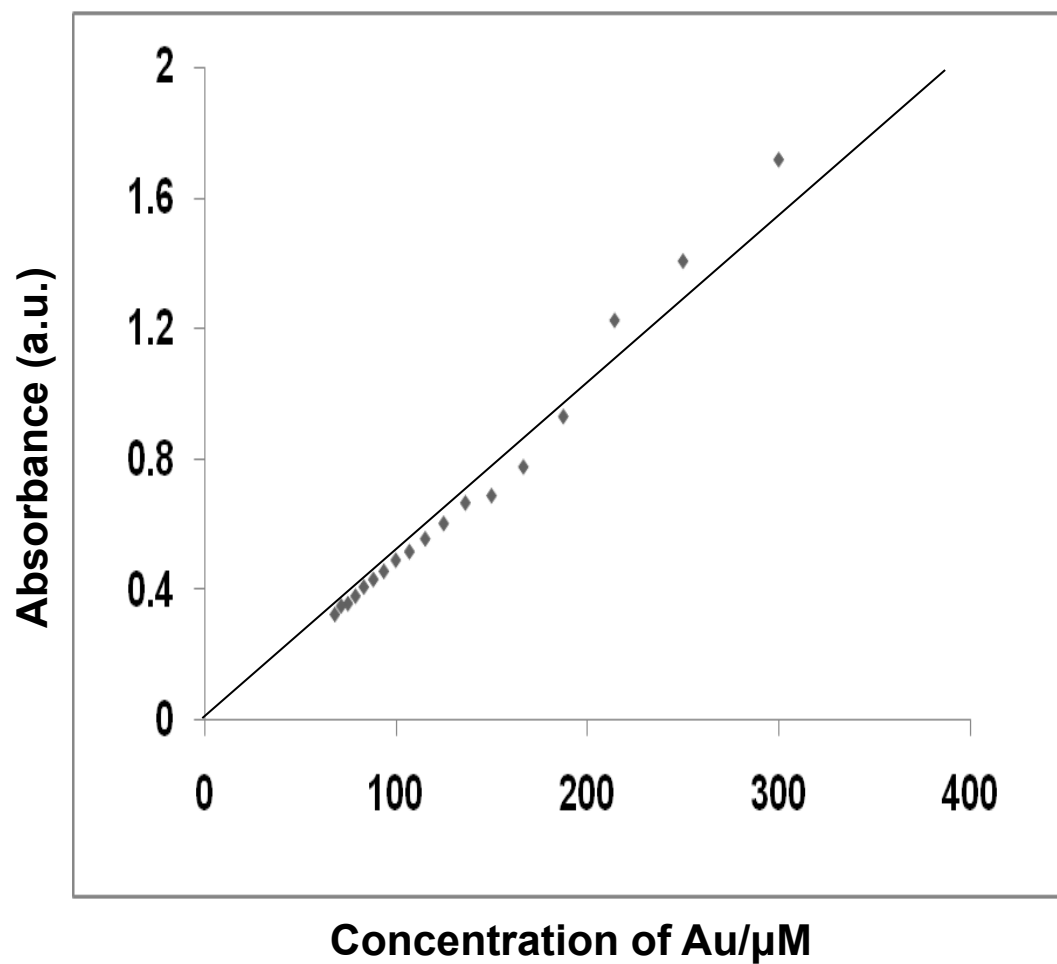
SI.Fig-7.(a-b): FTIR spectra of Olax leaf extract and AuNPs-OX-500. FTIR spectra of (a) *Olax Scandens* extract (OX) and (b) as synthesized gold nanoparticle by *Olax Scandens* extract (AuNP-OX-500) (Expt. No. #3 in Table-1). Relative transmittance abscissa: Wave number (cm⁻¹). FTIR spectra indicate the presence of polyphenols, aldehydes and proteins in Olax extract that help for the synthesis and stabilization of AuNPs-OX.

SI-Fig.8



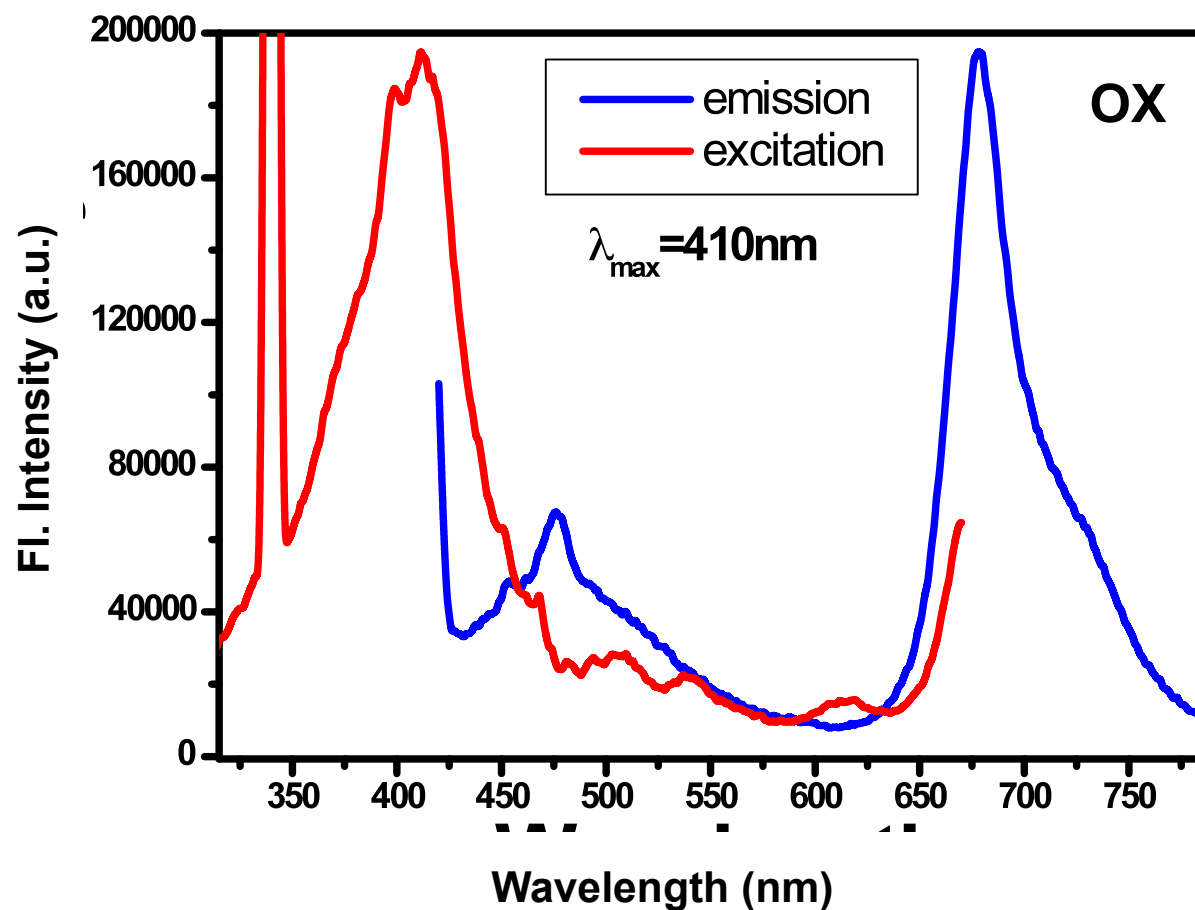
SI.Fig-8: SDS PAGE profile of *Olax* leaf extract and supernatant of AuNPs-OX-500 with silver nitrate staining. M indicates the standard protein marker. Lane-1 and -2 indicate the *Olax* extract and supernatant of AuNP-OX-500 obtained after centrifugation. The silver nitrate lane staining after gel electrophoresis shows the presence of low (12-17 kDa) molecular weight proteins in only *Olax* extract in lane-1 and disappearance of 12-17 kDa proteins in *Olax* extract associated with AuNPs in lane-2. The results confirm the role of low molecular weight proteins (12-17 kDa) for the formation and stabilization of AuNPs-OX.

SI-Fig.9



SI.Fig-9. : Effect of plasmon absorption of AuNP-OX-500. Change in the plasmon absorption of AuNP-OX-500 under various dilution conditions with water. Linear fit supports the extra stability of AuNP-OX-500 agrees with Lambert Beers law.

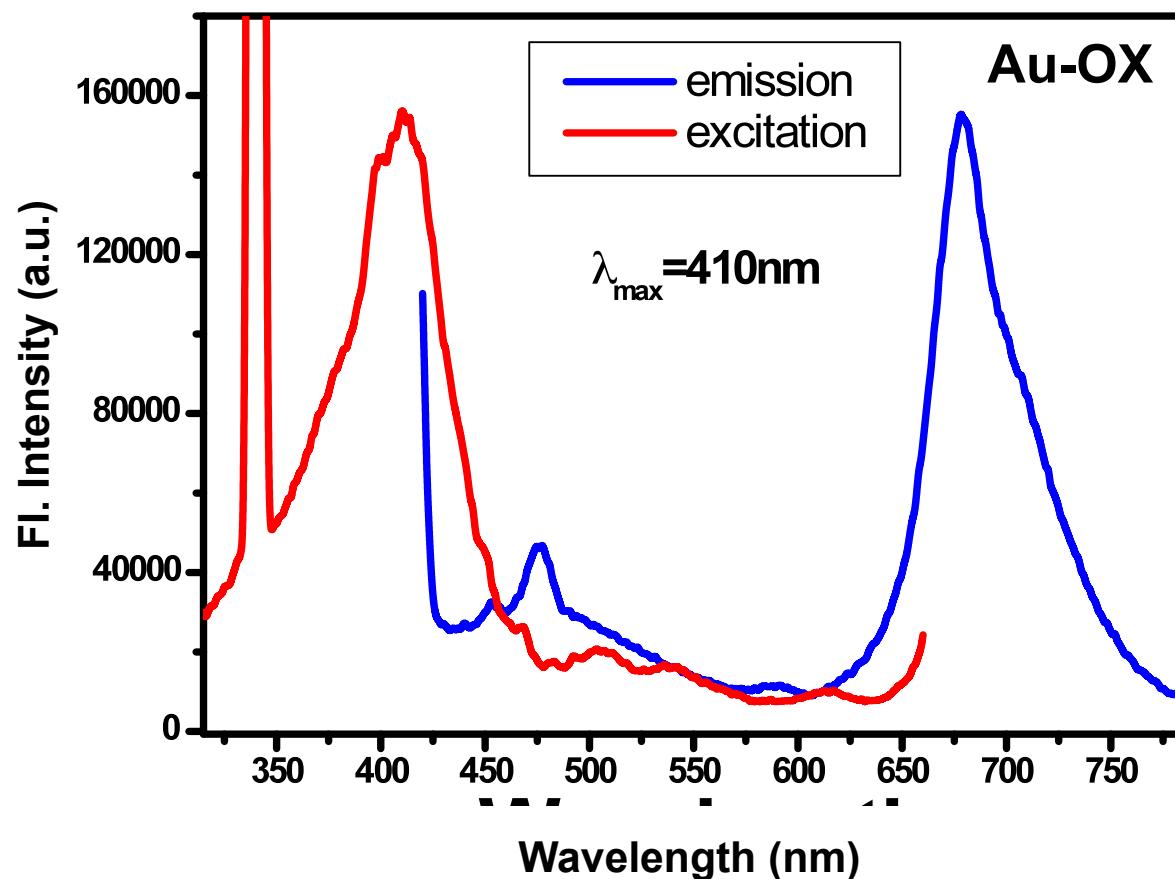
SI.Fig-10.a



SI.Fig-10 (a-c): Photoluminescence spectrums of Olax and AuNP-Ox-500.

(a) Blue line represents the photoluminescence emission spectra (emission spectrums show $\lambda_{\text{Em}} = 670\text{ nm}$) of Olax having excited at $\lambda_{\text{Ex}} = 410\text{ nm}$ which is showing by the red line.

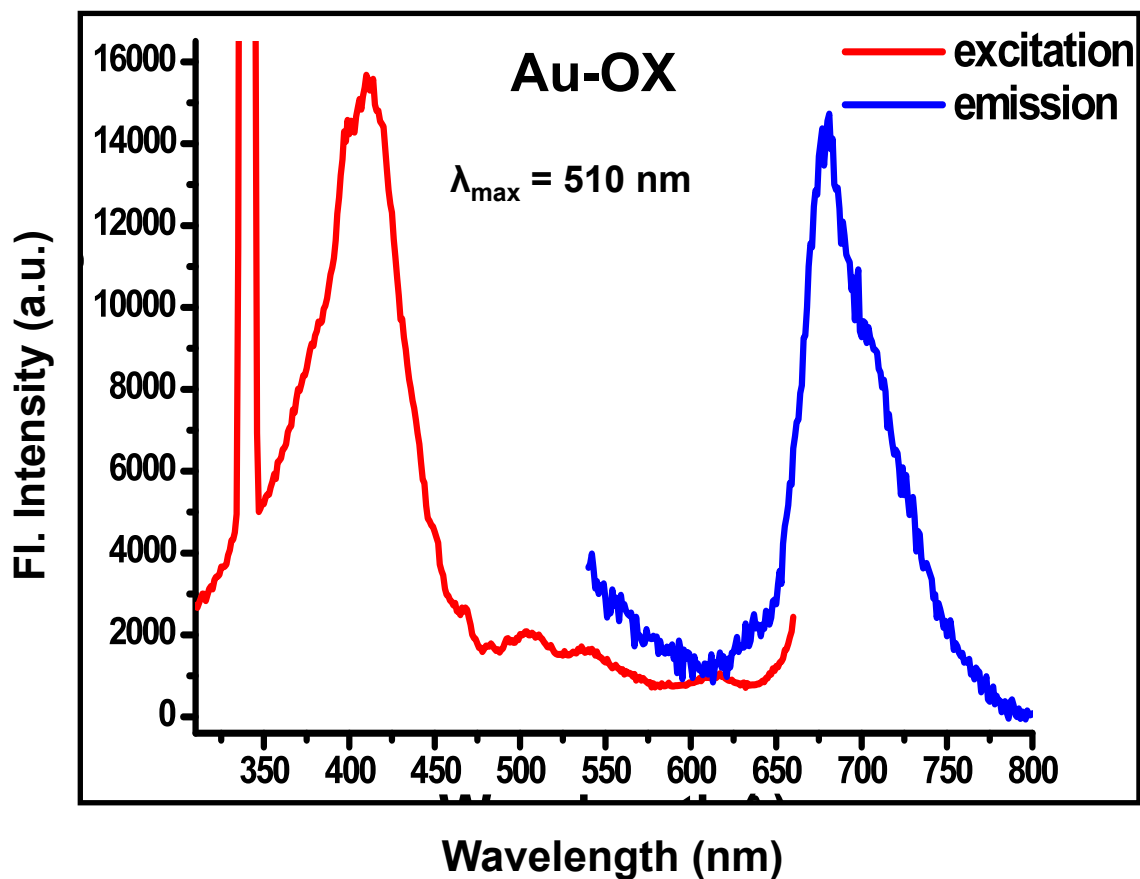
SI.Fig-10.b



SI.Fig-10 (a-c): Photoluminescence spectrums of Olax and AuNP-Ox-500.

(b) Blue line represents the photoluminescence emission spectra (emission spectrums show $\lambda_{\text{Em}} = 670\text{ nm}$) of AuNP-Ox-500 having excited at $\lambda_{\text{Ex}} = 410\text{ nm}$ which is showing by the red line.

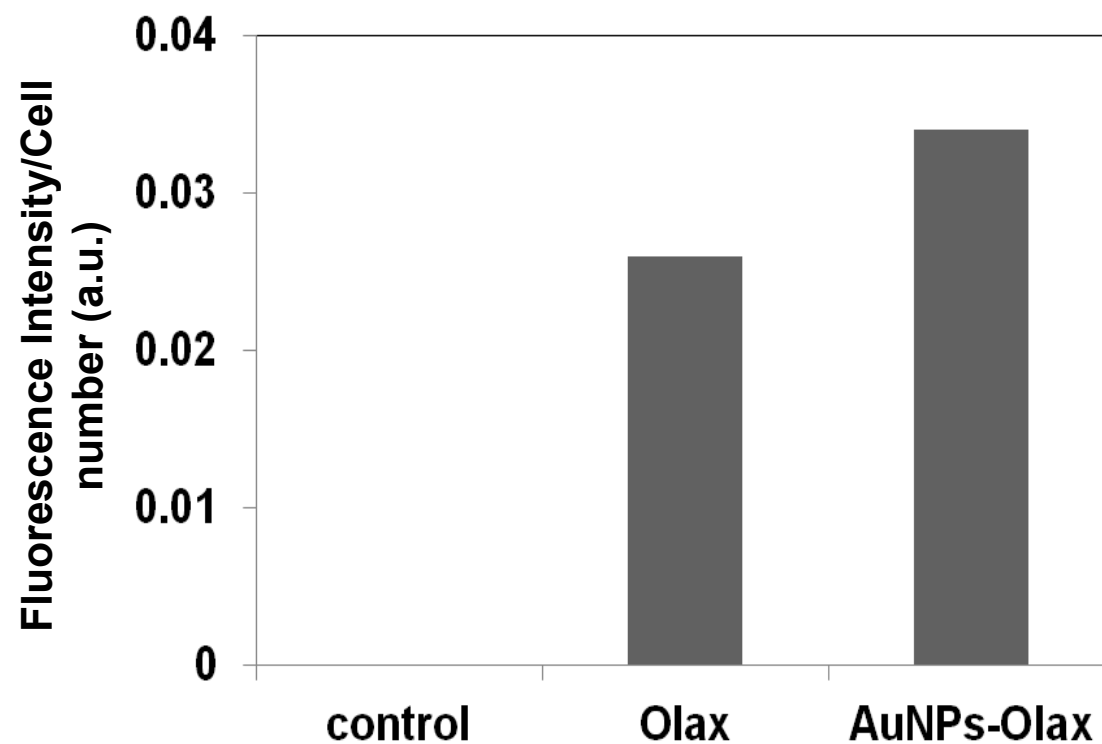
SI.Fig-10.c



SI.Fig-10 (a-c): Photoluminescence spectrums of Olax and AuNP-Ox-500.

(c) Blue line represents the photoluminescence emission spectra (emission spectrums show $\lambda_{\text{Em}} = 670 \text{ nm}$) of AuNP-Ox-500 having excited at $\lambda_{\text{Ex}} = 510 \text{ nm}$ which is showing by the red line.

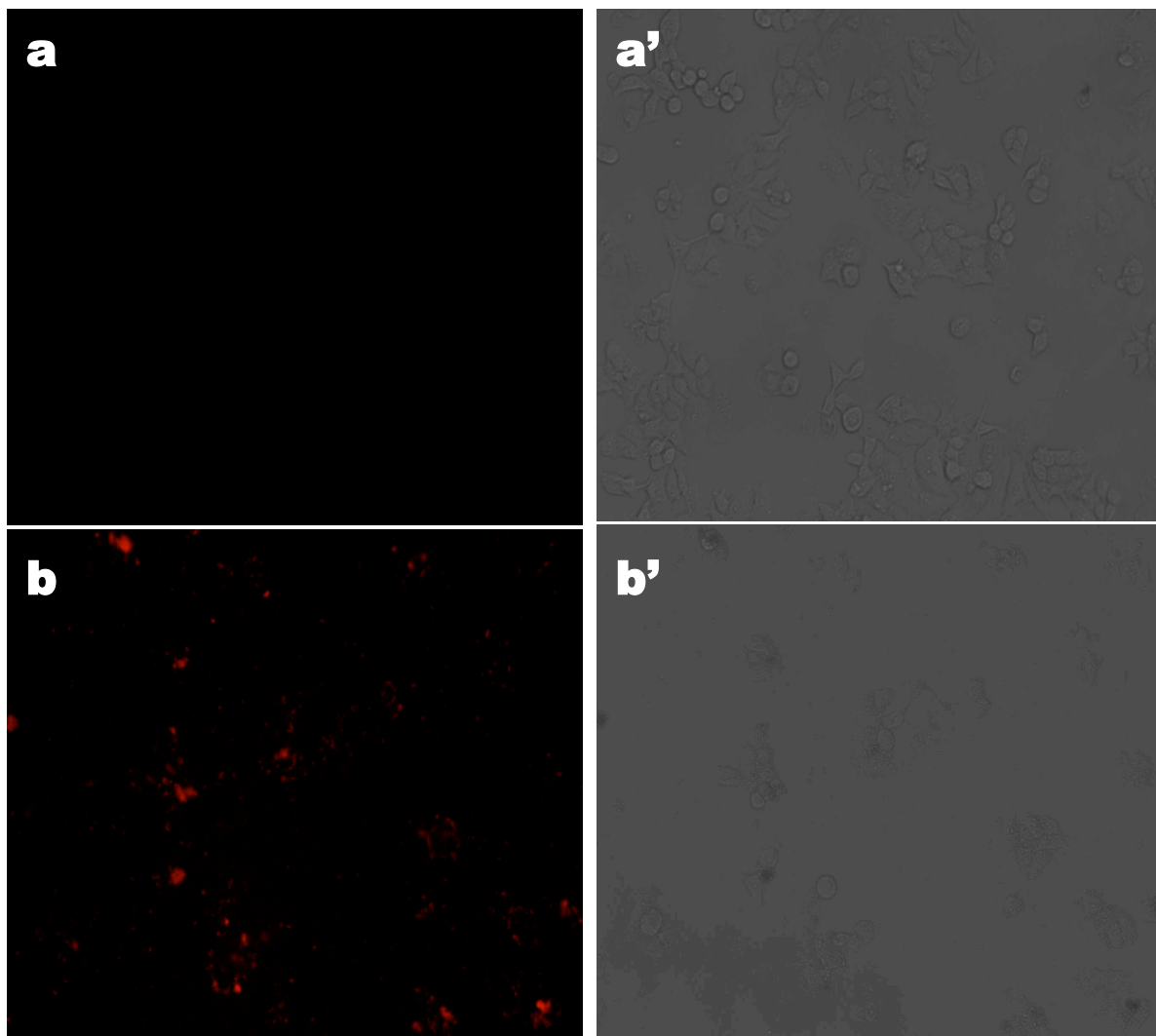
SI.Fig-11



SI.Fig-11 : Normalisation of fluorescence intensity. Plot of fluorescence intensity/cell numbers (a.u.) vs untreated, cell treated by Olax and cell treated by AuNPs-Olax shows that AuNPs-Olax shows more intensity than Olax itself.

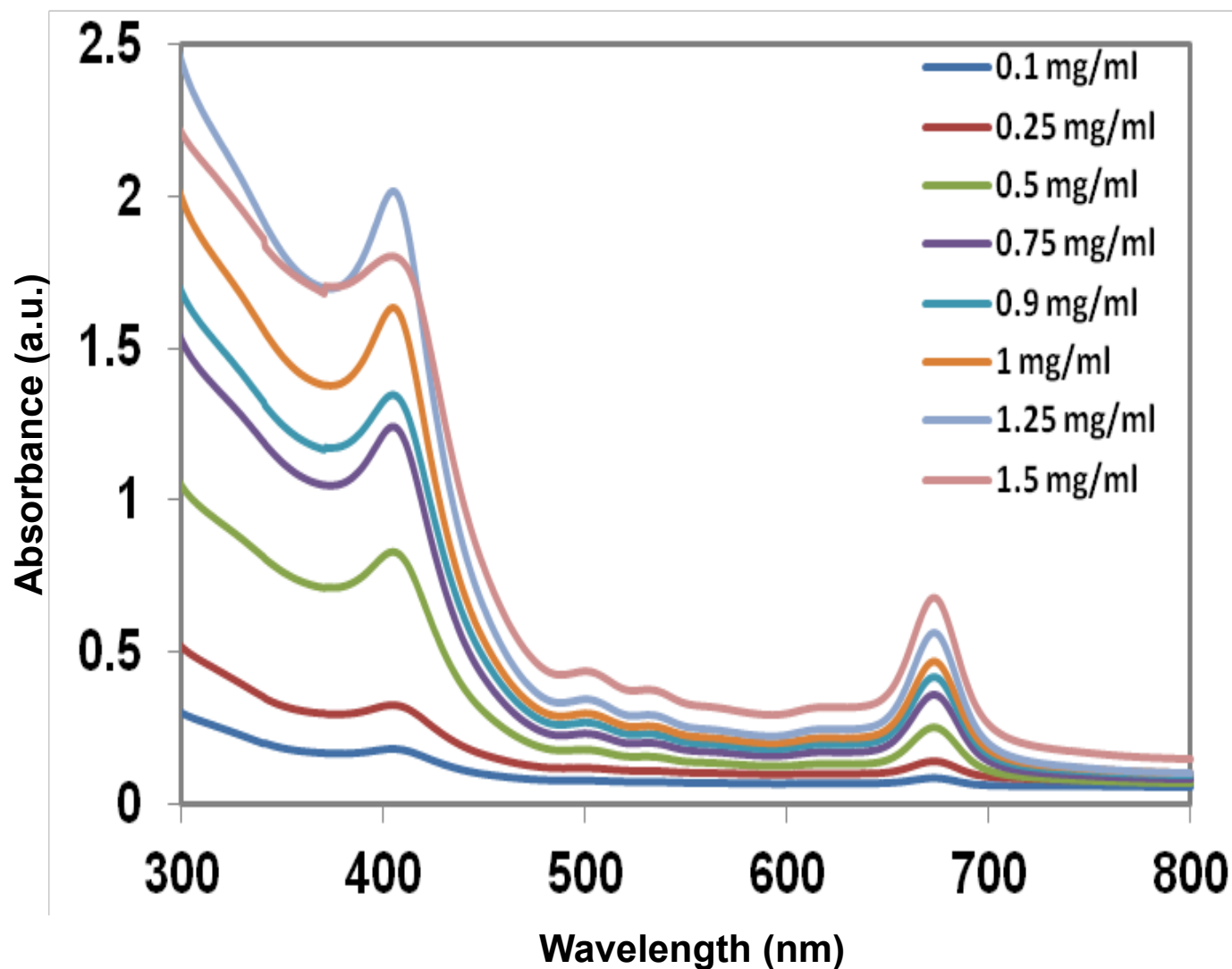
SI.Fig-12

MCF-7



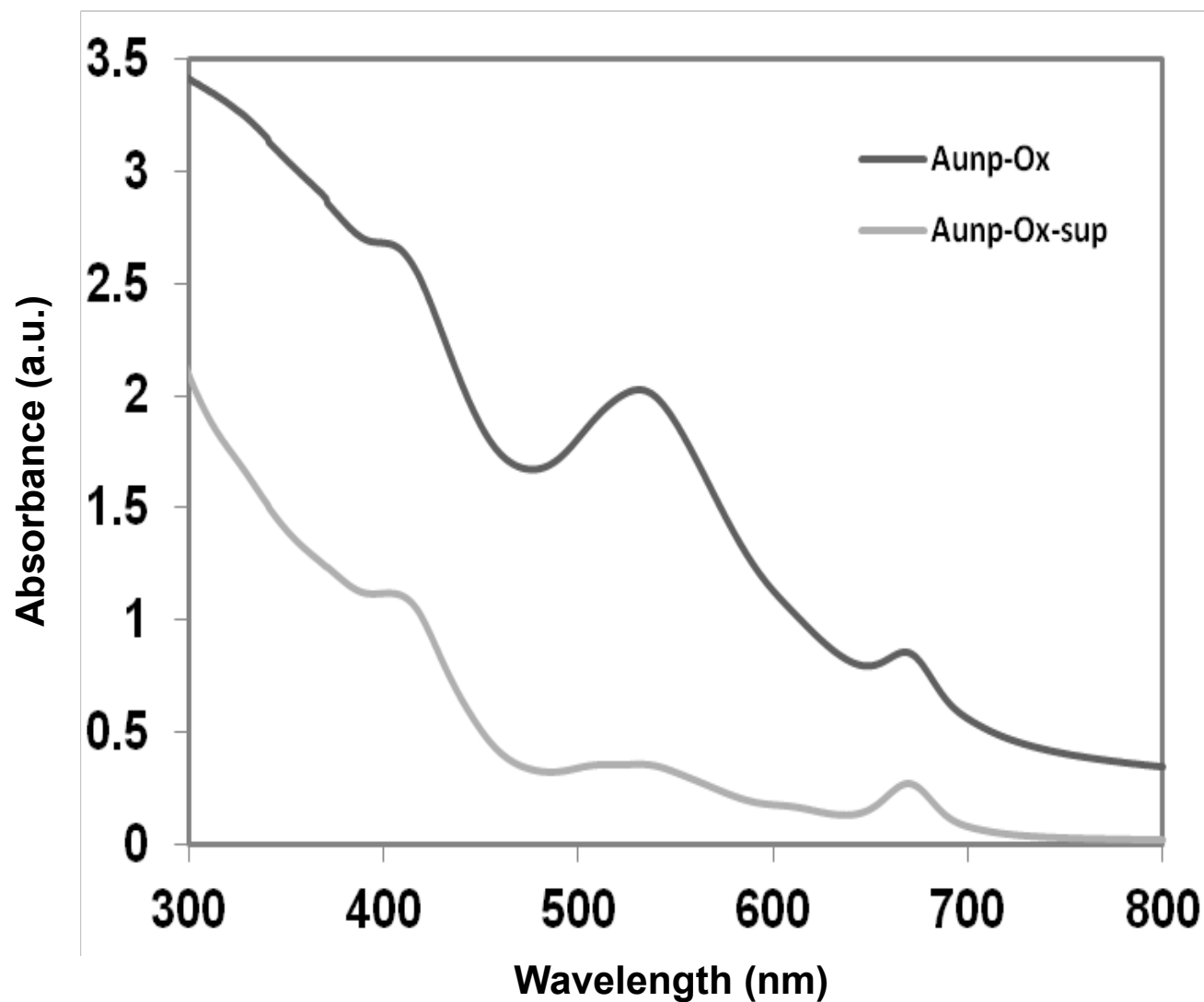
SI.Fig-12 (a-d): Fluorescence (a and b) and the corresponding phase images of (a' and b') MCF-7 cells untreated and treated with AuNP-Ox-500, observed by Olympus Fluorescence Microscope. (a and a'): fluorescence images of untreated MCF-7 cells and its corresponding phase image, (b and b'): fluorescence image of MCF-7 cells treated with AuNP-Ox-500 and its corresponding phase image. The AuNP-Ox-500 treated MCF-7 cells were extensive washing with DPBS (6 times) before taking the fluorescence images.

SI.Fig-13



SI.Fig-13: UV visible spectra of Olax in different concentration. The picture shows wavelength vs absorbance plots of DOX in aqueous solution for different concentrations starting from 0.1mg/ml to 1.5 mg/ml.

SI.Fig.14



SI.Fig-14: UV visible spectrums of AuNP-Ox-500 and supernatant of the same after centrifugation. The picture shows wavelength vs absorbance plots of AuNP-Ox-500 and supernatant of it after centrifugation.